Bis(κ^{2}S,S′-di(isopropyl)dithiocarbamato)nickel(II): anagostic C-H···Ni interactions and physical properties

Alexander Angeloski[a], Anthony Thomas Baker[b], Mohan Bhadbhade[c], Andrew Michael McDonagh[a]*,

[a]*School of Mathematical and Physical Sciences, University of Technology, Sydney 2007, Australia*
[b] *College of Science, Health and Engineering, La Trobe University, Melbourne 3086, Australia*
[c]*School of Chemistry, The University of New South Wales, Sydney 2052, Australia*

Abstract

The molecular structure of bis(κ^2*S*,*S*′-di(isopropyl)dithiocarbamato)nickel(II) has been examined by single crystal X-ray diffraction. The data reveal a C-H···Ni anagostic interaction arising from the interaction of two non-equivalent molecules within the crystal. Thermal analysis data show that the complex decomposes at ~330 °C. The structure of the resultant NiS material was examined using scanning electron microscopy and energy dispersive X-ray spectroscopy which revealed NiS nanowires.

"Keywords: Dithiocarbamate; Anagostic; Square-planar nickel(II); FTIR; NMR; XRD"

1. Introduction

Dithiocarbamate complexes have attracted a significant amount of attention due to their ease of synthesis, the ability to coordinate to a range of transition and main block elements, and their interesting and useful properties.[1-3] The combination of various metal centres with the sizeable range of substituted dithiocarbamate ligands has yielded complexes with applications such as anti-neoplastic agents,[4] rescue agents in cisplatin therapy,[5] bioanalytical agents[6] as well as single source precursors of metal sulfide nanoparticles.[7] Dithiocarbamate complexes have also been investigated for the development of new sensors, IR detectors and solar cell technologies.[8] Substitution of the dithiocarbamato ligand gives rise to a range of electronic and steric effects across associated complexes. Some synthetic efforts have focused on optimising ligand design to allow for altered thermal properties required for nanoparticle synthesis.[9] Thus, dithiocarbamate complexes containing heterocyclic,[10] alkyl[11] and phenyl[12] ligands have been pursued as single source nanoparticle precursors.

In the context of structural interactions and possible applications of metal dithiocarbamate complexes, we have revisited the synthesis and spectroscopic characterisation of bis(κ^2*S*,*S*′-di(isopropyl)dithiocarbamato)nickel(II) and herein report a packing polymorph of the title compound showing anagostic interactions. There are few reported structural determinations for diisopropyldithiocarbamato (i-PrDTC) complexes with the only examples being Au(i-Pr$_2$DTC)$_2$, Pb(i-Pr$_2$DTC)$_2$, Hg(i-Pr$_2$DTC)$_2$ and Ni(i-Pr$_2$DTC)$_2$.[13-16]

* Corresponding author. Tel.: +61-2-9514-1035.
E-mail address: Andrew.McDonagh@uts.edu.au

2. Experimental

2.1. Reagents and Instruments

Chemicals and solvents used in synthetic procedures were analytical or reagent grade and purchased from Sigma Aldrich and used as received. Millipore water (18.4 MΩ cm^{-1}) was used in synthetic procedures. FT-IR spectra of single crystals were recorded using an Agilent Cary 630 FTIR spectrometer fitted with a ZnSe ATR accessory. Each spectrum was collected using 16 scans, with a resolution of 4 cm^{-1} over the range of 4000 to 700 cm^{-1}.

Proton and carbon nuclear magnetic resonance spectroscopy was performed using an Agilent Technologies NMR instrument operating at 500.3 MHz (for ^{1}H experiments) and 125.7 MHz (for ^{13}C experiments) at 25 °C. ^{1}H experiments were acquired using 16 scans with a 0.01 s relaxation delay and a pulse angle of 60 °. For ^{13}C experiments, 300 scans with a 1.00 s relaxation delay and a pulse angle of 45 ° were used. The title compound was dissolved in deuterated chloroform and the solvent residual chemical shifts of 7.26 ppm (for ^{1}H experiments) and 77.0 ppm (for ^{13}C experiments) were used to calibrate the spectra. Compound **1** was dissolved in deuterated methanol and the solvent residual chemical shifts of 3.31 ppm (for ^{1}H experiments) and 49.0 ppm (for ^{13}C experiments) were used to calibrate the spectra. High resolution mass spectra were acquired using an Agilent 6510 Q-TOF with a mobile phase of 65% acetonitrile, 35% water.

UV-Vis spectra of $CHCl_3$ solutions (8.3×10^{-5} mol L^{-1}) were recorded using an Agilent 8453 spectrometer. The spectra were collected from 190 to 1100 nm using a resolution of 1 nm. A Thermal Advantage SDT-Q600 thermal analyser was used to obtain TG, DTG and DSC data simultaneously using alumina crucibles. Experiments were conducted using a flow of nitrogen gas (150 ml min^{-1}) and a heating rate of 10 °C min^{-1} over a temperature range of 25 – 500 °C. Residues from TGA experiments were imaged using a Zeiss Supra 55VP SEM and a Zeiss EVO LS15 SEM fitted with a Bruker Nano EDX detector was used for EDX microanalysis.

2.2. Crystallographic analysis

Suitable single crystals of **2** (Scheme 1) were selected under a polarizing microscope (Leica M165Z), mounted on a MicroMount (MiTeGen, USA) consisting of a thin polymer tip with a wicking aperture. The X-ray diffraction measurements were carried out on a Bruker kappa-II CCD diffractometer at 150 K using an IμS Incoatec Microfocus Source with Mo-Kα radiation (λ = 0.710723 Å) . The single crystal, mounted on the goniometer using cryo loops for intensity measurements, was coated with paraffin oil and then quickly transferred to the cold stream using an Oxford Cryo stream attachment. Symmetry related absorption corrections using the program SADABS[17] were applied and the data were corrected for Lorentz and polarisation effects using Bruker APEX2 software.[18] The structure was solved by direct methods and the full-matrix least-squares refinement was carried out using Shelxl [19] in Olex2.[20] The non-hydrogen atoms were refined anisotropically. The molecular graphic was generated using Olex2.[20] Packing diagrams were generated using the program Mercury.[21]

2.3. Synthesis

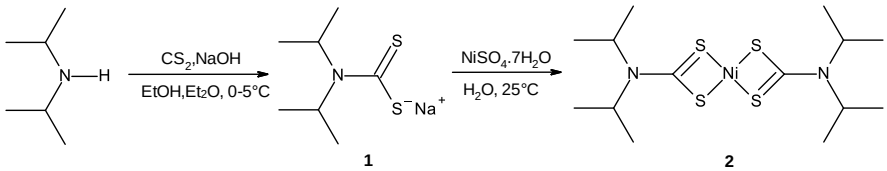

Scheme. 1. Synthesis of **1** and **2**.

*Synthesis of sodium di(isopropyl)dithiocarbamate (**1**):* Compound **1** (Scheme 1) was prepared using an adaptation of the method of Shinobu *et al.*[22] An aqueous solution of sodium hydroxide (4.00 g in 10 mL) was cooled with stirring to 0 °C. Diisopropylamine (10 mL) was added followed by diethyl ether (120 mL). The solution was maintained at 5 °C whilst carbon disulfide (10 mL in 5 mL of ethanol) was added dropwise. A precipitate formed immediately upon addition and the resultant mixture was stirred for 30 minutes. The crude product was collected by filtration and purified by recrystallisation of a saturated methanolic solution by slow diffusion of diethyl ether. The colourless crystals were collected by filtration, washed with cold diethyl ether, and dried over P_2O_5 *in vacuo*. The ligand crystalises with two waters of hydration as shown by TGA. HRMS $(M+H)^+$ for $NaNS_2C_7H_{14}$ Calculated: 200.0538; Found: 200.0549. ^{1}H NMR (500.3 MHz, CD_3OD): δ 6.24 (br.s, 1H, C***H***$(CH_3)_2$), 3.88 (br.s, 1H, C***H***$(CH_3)_2$), 1.68 (br.s, 6H, CH(C***H*****3**$)_2$), 1.17 (br.s, 6H, CH(C***H*****3**$)_2$). ^{13}C NMR (125.7 MHz, CD_3OD): δ 211.2 (N***C***S_2), 57.5 (N***C***$(CH_3)_2$), 51.0 (N***C***$(CH_3)_2$), 21.3 (C(***C***$H_3)_2$), 19.8 (C(***C***$H_3)_2$).

Synthesis of bis(κ^{2}S,S'-di(isopropyl)dithiocarbamato)nickel(II) (**2**):An aqueous solution of compound **1** (3.00 g, 13 mmol, in 10 mL of water) was added to an aqueous solution of nickel sulfate heptahydrate (1.46 g, 5 mmol in 8 mL of water). A dark green precipitate formed immediately upon addition. The precipitate was filtered, washed with ice cold water and then diethyl ether, and dried over P_2O_5 *in vacuo* to yield 1.77 g of **2** (86%). Crystals suitable for X-ray analysis were obtained as dark green blocks from solvent counter diffusion of diethyl ether into a chloroform solution of **2** over two days. HRMS $(M+H)^+$ for $NiN_2S_4C_{14}H_{28}$ Calculated: 411.0562; Found: 411.0566. ^{1}H NMR (500.3 MHz, $CDCl_3$): δ 4.56 (br.s, 2H, C***H***$(CH_3)_2$), 1.38 (br.s, 12H, CH(C***H*****3**$)_2$. ^{13}C NMR (125.7 MHz, $CDCl_3$): δ 205.8 (N***C***S_2), 50.9 (N***C***$(CH_3)_2$), 19.7 (C(***C***$H_3)_2$) UV ($CHCl_3$, ε (L M^{-1} cm^{-1}): λ 618 (76), 490 (268), 435 (1581), 400 (5840), 330 (32100).

3. Results and discussion

3.1. X-ray Crystal Structure Determination

Table 1. Crystal data and structure refinement parameters for **2**.

Chemical formula	$2(C_7H_{14}NNi_{0.5}S_2)$
M_r	411.33
Crystal system, space group	Monoclinic, $P2_1/c$
Temperature (K)	150
a, b, c (Å)	8.1195 (4), 17.6976 (8), 14.6740 (8)
β (°)	102.631 (3)
V (Å^3)	2057.56 (18)
Z	4
Radiation type	Mo $K\alpha$
μ (mm^{-1})	1.34
Crystal size (mm)	0.27 × 0.17 × 0.06
Absorption correction	Multi-scan *SADABS2014*/5[17] was used for absorption correction. wR2(int) was 0.1124 before and 0.0506 after correction. The Ratio of minimum to maximum transmission is 0.8221. The λ/2 correction factor is 0.00150.
T_{min}, T_{max}	0.613, 0.746
No. of measured, independent and observed [$I > 2\sigma(I)$] reflections	17808, 4534, 3879
R_{int}	0.037
$(\sin \theta/\lambda)_{max}$ (Å^{-1})	0.643
$R[F^2 > 2\sigma(F^2)]$, $wR(F^2)$, S	0.027, 0.070, 1.03
No. of reflections	4534
No. of parameters	201
H-atom treatment	H-atom parameters constrained
$\Delta\rangle_{max}$, $\Delta\rangle_{min}$ (e Å^{-3})	0.46, -0.26

Table 2. Selected bond lengths (Å) and angles (°) for **2**.

Bond Lengths			
Ni1B—S1B	2.1892 (4)	Ni1A—S1A	2.1965 (4)
Ni1B—S1B^{i}	2.1891 (4)	Ni1A—S1A^{ii}	2.1965 (4)
Ni1B—S2B^{i}	2.1870 (4)	Ni1A—S2A^{ii}	2.1912 (4)
Ni1B—S2B	2.1870 (4)	Ni1A—S2A	2.1912 (4)
S1B—C1B	1.7241 (16)	S1A—C1A	1.7267 (17)
S2B—C1B	1.7263 (15)	S2A—C1A	1.7294 (16)
N1B—C1B	1.314 (2)	N1A—C1A	1.316 (2)
N1B—C2B	1.493 (2)	N1A—C2A	1.4933 (19)
N1B—C5B	1.490 (2)	N1A—C5A	1.490 (2)
C2B—C3B	1.512 (3)	C2A—C3A	1.519 (2)
C2B—C4B	1.517 (3)	C2A—C4A	1.520 (3)
C5B—C6B	1.517 (3)	C5A—C6A	1.524 (2)
C5B—C7B	1.521 (3)	C5A—C7A	1.521 (2)
Bond Angles			
S1B^{i}—Ni1B—S1B	180.000 (18)	S1A^{ii}—Ni1A—S1A	180.0
S2B—Ni1B—S1B^{i}	100.693 (15)	S2A—Ni1A—S1A^{ii}	100.834 (16)
S2B^{i}—Ni1B—S1B	100.692 (15)	S2A^{ii}—Ni1A—S1A	100.833 (15)
S2B—Ni1B—S1B	79.307 (15)	S2A—Ni1A—S1A	79.166 (15)
S2B^{i}—Ni1B—S1B^{i}	79.308 (15)	S2A^{ii}—Ni1A—S1A^{ii}	79.167 (15)
S2B^{i}—Ni1B—S2B	180.0	S2A^{ii}—Ni1A—S2A	180.0
C1B—S1B—Ni1B	86.30 (5)	C1A—S1A—Ni1A	86.35 (5)
C1B—S2B—Ni1B	86.32 (5)	C1A—S2A—Ni1A	86.46 (6)
C1B—N1B—C2B	123.67 (14)	C1A—N1A—C2A	119.68 (14)
C1B—N1B—C5B	119.73 (13)	C1A—N1A—C5A	123.66 (13)
C5B—N1B—C2B	116.59 (13)	C5A—N1A—C2A	116.65 (12)
S1B—C1B—S2B	108.07 (9)	S1A—C1A—S2A	107.99 (9)
N1B—C1B—S1B	127.36 (12)	N1A—C1A—S1A	125.09 (12)
N1B—C1B—S2B	124.57 (12)	N1A—C1A—S2A	126.92 (13)
N1B—C2B—C3B	112.38 (16)	N1A—C2A—C3A	110.40 (14)
N1B—C2B—C4B	111.17 (16)	N1A—C2A—C4A	110.51 (14)
C3B—C2B—C4B	114.13 (17)	C3A—C2A—C4A	113.02 (14)
N1B—C5B—C6B	110.59 (16)	N1A—C5A—C6A	112.38 (14)
N1B—C5B—C7B	110.19 (16)	N1A—C5A—C7A	112.14 (13)
C6B—C5B—C7B	113.79 (16)	C7A—C5A—C6A	113.45 (15)

Symmetry codes: (i) *-x*, *-y*, *-z*+1; (ii) *-x*, *-y*+1, *-z*+1.

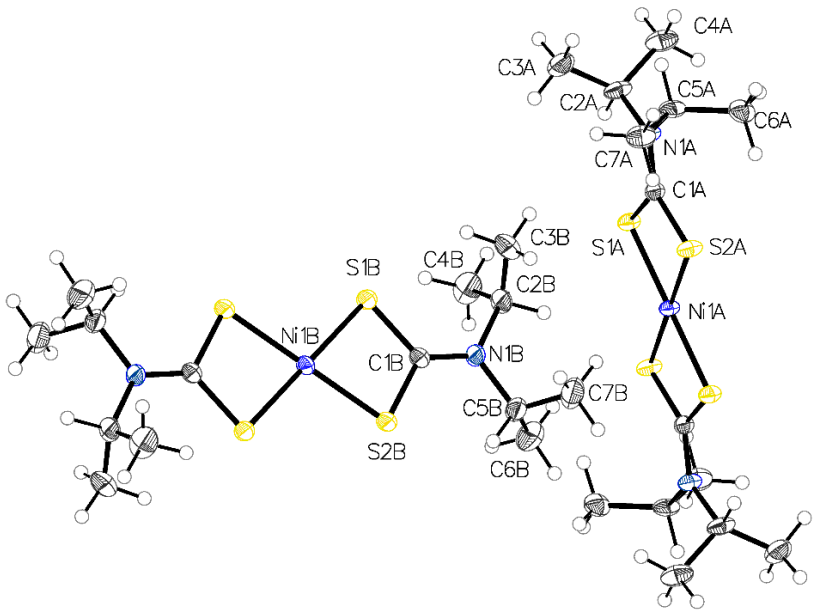

Fig. 1. ORTEP of **2** with atom labeling scheme and 50% thermal ellipsoids.

Relevant crystal data, selected bond lengths and angles are given in Tables 1 and 2. Analysis of the X-ray crystal structure reveals some interesting differences compared to previously reported data for this compound.[13, 23] In the current study, there are two independent molecules in the asymmetric unit (Figure 1). There are no significant differences in bond lengths, angles or intermolecular interactions between the current and previous structural determinations. The nickel atoms, Ni1A (molecule A) and Ni1B (molecule B) are located at centrosymmetric special positions at (0,0,0.5) and (0,0.5,0.5), respectively. There are no significant differences between corresponding bond lengths and bond angles in the two independent molecules. Both NiS_4 environments are approximately square planar, however there is a significant difference in the torsion angles about the Ni-S-C-S coordination centre; 1.69 (6)º for Ni1A—S1A—C1A—S2A and 0.23 (7)º for Ni1B—S1B—C1B—S2B. The geometry about N1A is close to planar (C5A—N1A—C1A—S2A = 0.2 (2)º) while the geometry about N1B deviates somewhat from planarity (C5B—N1B—C1B—S2B = -3.7 (2)º).

Table 3. Summary of previous and current unit cell parameters

Cell Volume (Å³)	a (Å)	b (Å)	c (Å)	β (º)	Reference
2127	8.160 (2)	17.830 (3)	15.620 (3)	110.50 (2)	[23]
2127.94	8.147 (2)	17.820 (2)	15.630 (2)	110.32 (3)	[13]
2057.56	8.119 (4)	17.698 (8)	14.674 (8)	102.63 (3)	This work

The unit cell parameters of **2** determined in the current work are summarized in Table 3 together with previously reported data for comparison.[13, 23] The unit cells are different with cell volumes, c axis lengths and β significantly smaller in the current study compared to the previous determinations. The differences between the current crystal structure and those previously reported are most apparent when viewed along the b axis (Figure 2). It is apparent that the differences in unit cells are the result of a difference in the relative rotation of molecules A and B. We propose that the differences in the current structure arise from different

solvent mixtures and methods used during the crystallisation process (chloroform/ethanol evaporation *vs* diffusion of diethyl ether into chloroform solution in the current report).

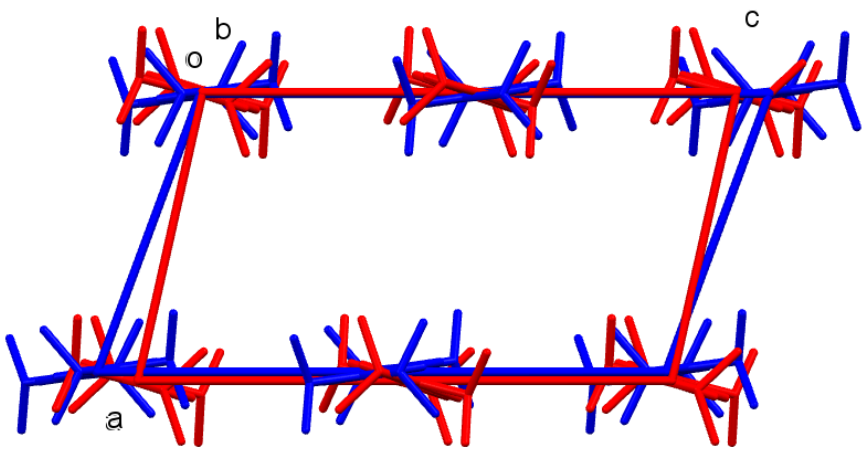

Fig. 2. Packing diagram showing a unit cell from previously determined structure[13] (blue) and unit cell (red) from the current structure viewed along the b axis (hydrogens and molecule A removed for clarity).

In the current study, molecule A is oriented in a perpendicular fashion to molecule B allowing for intermolecular H···S contacts, with H6BB (on C6B) approximately 3.09 Å from S2A. There is also an intermolecular H···S contact of approximately 2.90 Å between H5A (on C5A), and S2B. These intermolecular contacts are highlighted in Figure 3. In addition to the H···S contacts, there is a C-H···Ni contact of approximately 3.00 Å between H2B and Ni1A. Agostic and anagostic interactions[24] have been described for C-H···M interactions (where M is often a d^6 or d^8 metal).[25] Agostic interactions are 3-centre-2-electron interactions characterised by short H···M distances (≈ 1.8 – 2.2 Å) and C-H···M angles of 90 – 130°.[26] Anagostic interactions are characterised by longer H···M distances (≈ 2.3 – 3.0 Å) and C-H···M angles of 110 – 170°.[27] In the present case, the H···M distance of approximately 3.00 Å and C-H···Ni bond angle of ca. 160° is characteristic of an anagostic interaction between molecules A and B. Although such interactions have generally been reported as structural curiosities, they may play an important role in reactivity and involved in catalytic activity.[28]

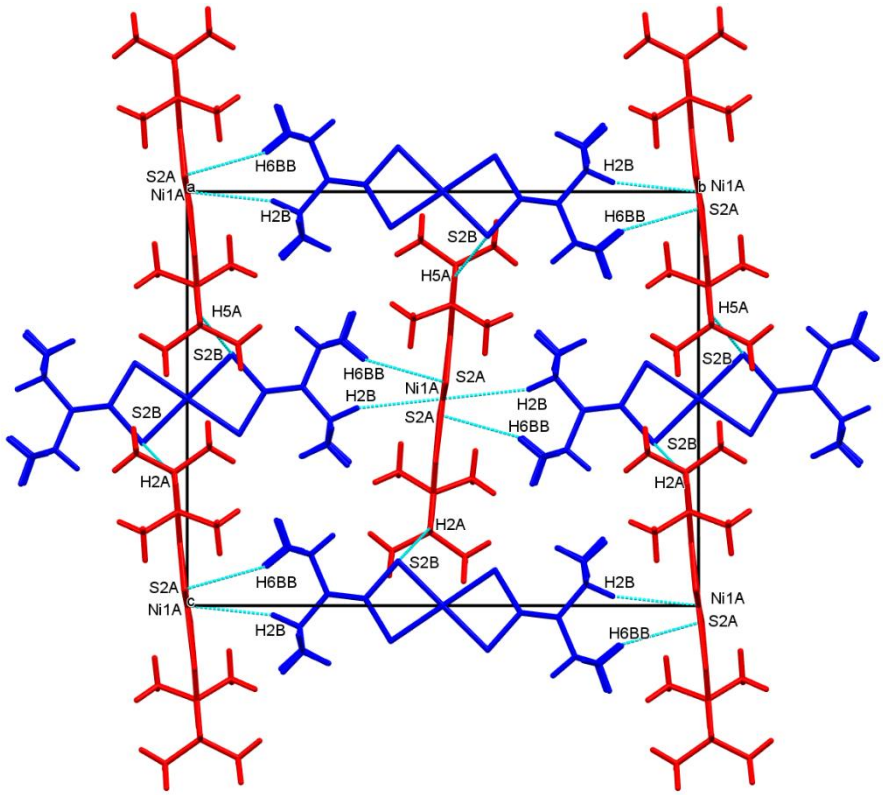

Fig. 3. Packing diagram depicting the Ni-H and S-H interactions along the a axis between molecule A (red) and molecule B (blue).

3.2. FT-IR and UV-VIS spectroscopy

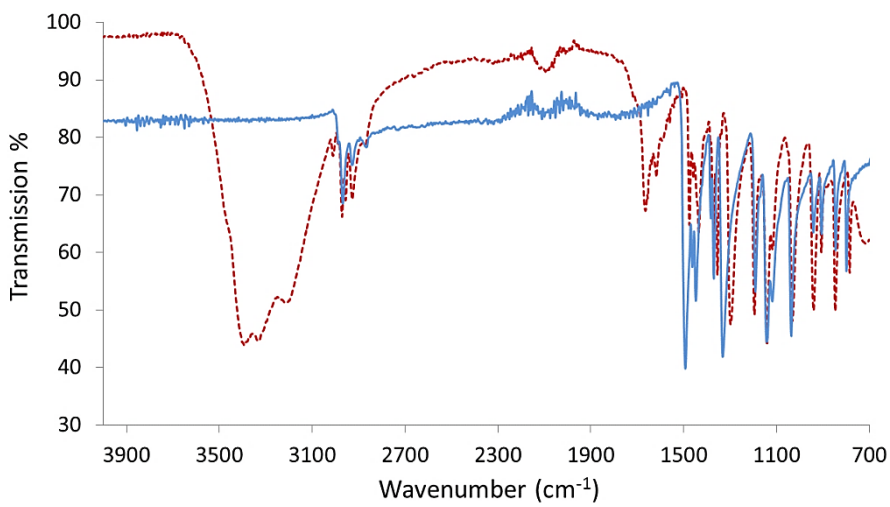

Fig. 4. FTIR spectra of **1** (red) and **2** (blue).

Table 4. Selected IR spectral data for **1** and **2** (cm^{-1}).[a]

Assignment	1	2
ν (O-H)	3300	N/A
ν (C-H)	2965	2963
δ (O-H)	1665	N/A
ν_s (C···N)	1472	1487
ν_{as} (CH_3)	1429	1437
ν_{sy} (CH_3)	1352	1364
ν (N-C)	1296	1327
ρ (CH_3)	1139	1139
ν_s (C···S)	936	938

[a] ν = stretching mode, δ = bending mode, ρ = rocking mode

IR data for **1** and **2** are presented in Figure 4, and relevant band assignments are summarized in Table 4. There are several notable differences between the spectra. The C···N stretch moves to higher energy by ~15 cm^{-1} upon coordination, which indicates an increase in the carbon-nitrogen bond order.[29] A single ν(C···S) band for each compound (936 and at 938 cm^{-1}, respectively) indicates that the two C···S bonds (within the NCS_2 moiety) are similar in nature.[30] The similar frequencies of the C···S bands for **1** and **2** suggest that the C···S bond lengths change little upon coordination of the ligand to the nickel(II) metal centre. There are two N-C stretching bands (C1-N1 and C2/C5-N1) in **1** and **2**. Upon coordination to nickel(II), both bands increase in frequency indicating shortened N-C bond lengths within the delocalised electron environment about the planar nitrogen. Bands at ~1430, 1350 and 1140 cm^{-1} are assigned to the asymmetric, symmetric and rocking vibrations of the methyl groups, respectively.[31] We assign the increase in the energies of the vibrations associated the CH_3 groups when moving from **1** to **2** to reduced molecular flexibility arising from Ni···H and S···H interactions. Bands below 900 cm^{-1} were not able to be unambiguously assigned due to vibrational mode coupling, most probably involving C-S stretches.[31] Another notable difference is the presence of O-H stretches and bends in **1**, which are attributed to water within the ligand matrix (as indicated by TGA data) but absent in the complex (as revealed by X-ray crystal data).

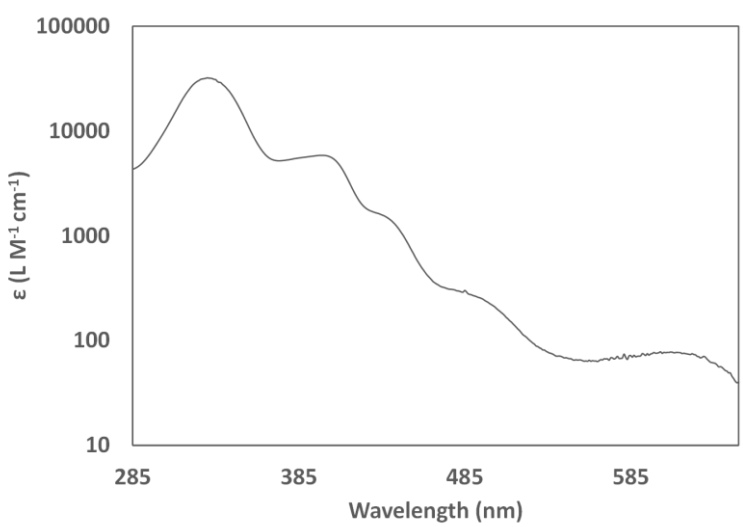

Fig. 5. Electronic spectrum of **2** in chloroform.

The electronic spectrum of **2** in chloroform (Figure 5) shows three broad d-d absorption transitions at 618 (ε = 76 L M^{-1} cm^{-1}), 490 (ε = 268 L M^{-1} cm^{-1}) and 435 nm (ε = 1581 L M^{-1} cm^{-1}). These bands are assigned to the $^1A_{1g} \rightarrow {}^1A_{2g}$, $^1A_{1g} \rightarrow {}^1B_{1g}$ and $^1A_{1g} \rightarrow {}^1E_g$ transitions respectively.[32-34] The presence of three d-d transition bands is characteristic for square planar d^8 nickel(II) complexes, and in agreement with the crystal structure of **2**.[33] The spectrum also shows an intense ligand to metal charge-transfer band at 330 nm (ε = 32124 L M^{-1} cm^{-1})[33, 35, 36] as well as an intense band at 400 nm (ε = 5844 L M^{-1} cm^{-1}) which is assigned to $\pi \rightarrow \pi^*$ transitions within the ligand N-C=S moiety.[35]

3.3 ^1H and ^{13}C NMR studies

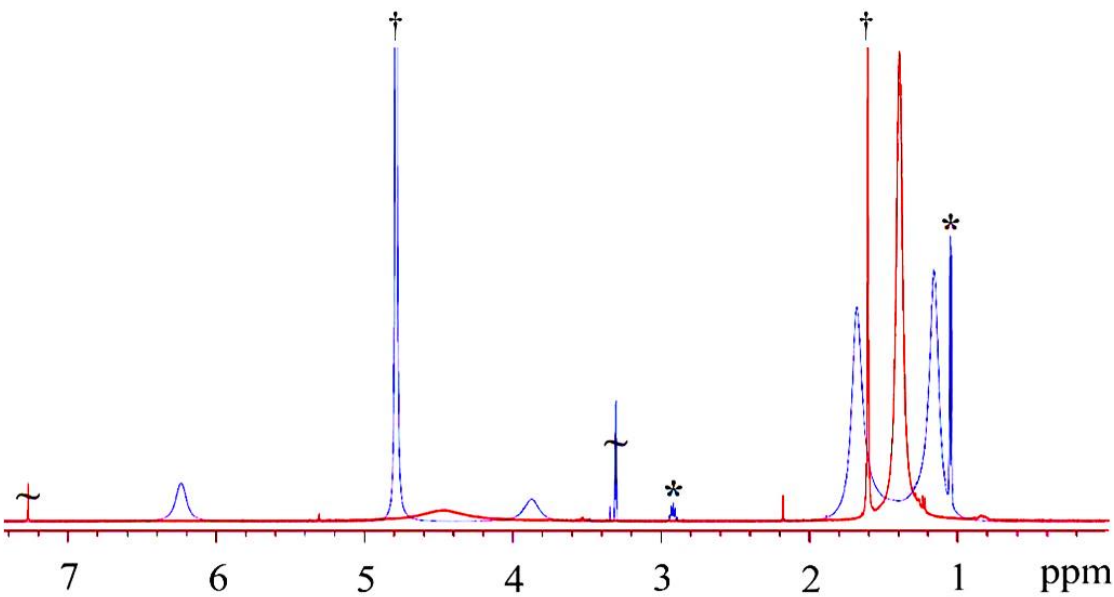

Fig. 6. ^1H NMR spectra for **1** (blue, solvent = CD_3OD) and **2** (red, solvent = $CDCl_3$), at 25 °C. ~ denotes solvent signal, * denotes residual diisopropylamine, † denotes residual H_2O.

^1H NMR spectra of **1** and **2** are shown in Figure 6. The spectrum of **1** shows two sets of peaks arising from the ligand protons, suggesting that the two isopropyl groups are inequivalent. A signal at 6.24 ppm is assigned to one of the methine protons while a signal at 3.88 ppm is assigned to the other. The different environments may arise due to C-H···S interactions.[27] Similarly, two resonances at 1.68 and 1.17 ppm are assigned to the methyl groups in two inequivalent environments. Similar observations have been observed in di(isopropyl)dithiocarbamato complexes [37, 38] and arise due to hindered rotation about an N-C bond (as a result the aforementioned C-H···S interaction) creating two magnetically inequivalent environments.[37-39] The ^1H NMR spectrum of **2** contains only one signal arising from the methine protons and one signal for the methyl groups. This suggests that coordination to the metal centre diminishes the effect of C-H···S interactions. However, in the spectra of both **1** and **2**, the signals are broad, characteristic of underlying dynamic processes in solution. Signals assigned to C***H***(CH_3) in the spectrum of **2** appear as a broad singlet at 4.56 ppm, which is characteristic of protons associated with the H···Ni anagostic interaction.[27, 40, 41] Signals assigned to CH(C***H***$_3)_2$ protons appear at 1.38 ppm, which has previously been suggested as an indicator of interactions with the CS_2 moiety.[42] The change in the number of signals in the spectrum of **2** compared to that of **1** is attributed to a change in the intermolecular attractions in the solution state that occur upon coordination.

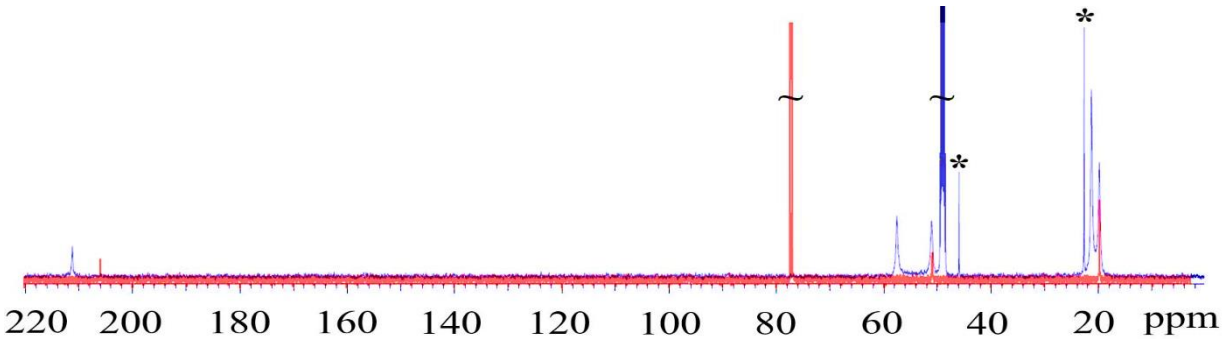

Fig. 7. ^{13}C NMR spectra for **1** (blue, solvent = CD_3OD) and **2** (red, solvent = $CDCl_3$), at 25 °C. ~ denotes solvent signal, * denotes residual diisopropylamine. The 90-190 ppm region has been omitted for clarity.

The ^{13}C NMR spectra show signals arising from each of the carbon atoms of **1** and **2** (Figure 7). The signals at δ 211.2 and δ 205.7 for **1** and **2,** respectively, are attributed to the N***C***S_2 moiety. An upfield shift of ~5.5 ppm upon moving from **1** to **2** is the result of increased electron density within the NCS_2 moiety,[43-45] which correlates with decreased C-N bond lengths revealed by FTIR spectroscopy. Two signals assigned to the methyl groups of **1**, as well as two signals for the methine carbon atoms are consistent with the assignments made for the ^{1}H NMR spectra. Similarly, fewer signals are observed in the spectrum of **2**.

3.4 Thermal and microstructural analysis

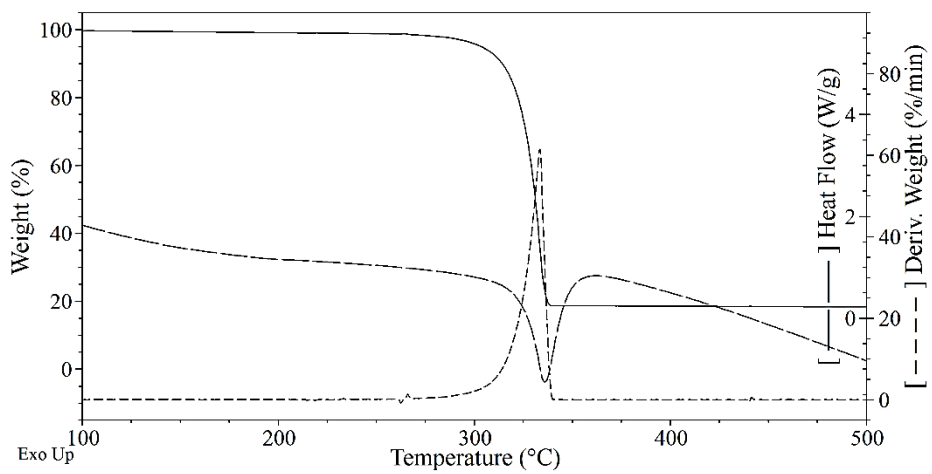

Fig. 8. TGA and DSC data for **2**. The 25-100 °C region has been omitted for clarity.

Thermogravimetric analysis (TGA) and differential scanning calorimetry (DSC) data for **2** are shown in Figure 8. There was insignificant mass loss in the region 25 - 120 °C, which indicates a lack of water (bound or otherwise) and is in agreement with the crystallographic data. Decomposition of **2** occurs in a single event between 298 °C and 340 °C with an endothermic peak at 333 °C corresponding to the loss of both ligands to produce the final decomposition product, NiS. The calculated mass loss for this event (78.1%) agrees with that observed (78.0%). The correlation between DTG_{max} and DSC_{max} suggests that thermal mass loss occurs at the onset of a solid-liquid phase change. This correlation has been commented on previously.[46]

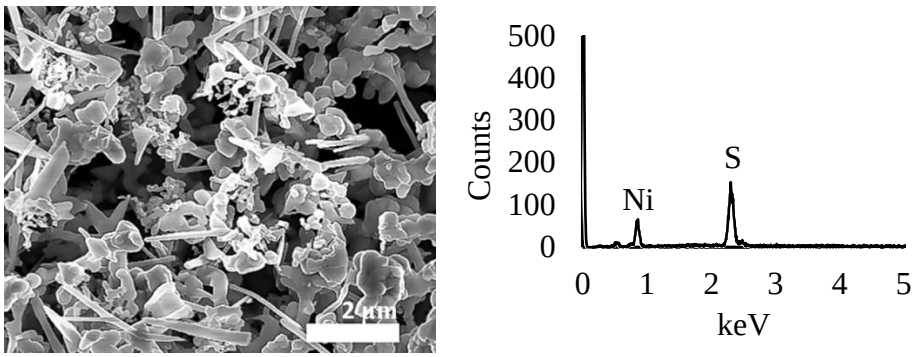

Fig. 9. SEM micrograph (a) and EDX plot (b) of the TGA residue from **2.**

Scanning electron microscopy analysis of the TGA residue from **2** was performed and a representative micrograph is shown in Figure 9. The material contains globular particles as well as rods with dimensions of ~0.15 x ~2 μm. Energy dispersive X-ray (EDX) analysis, Figure 9, shows that the residue contains nickel and sulfur only. This finding is in agreement with the assignment of the formula NiS for the thermolysis product. NiS nanowires obtained from the solid phase thermal decomposition of a dithiocarbamate precursor molecule have been hitherto not reported.

Conclusions

The molecular structure of single crystals of bis(κ^2*S*,*S*′-di(isopropyl)dithiocarbamato)nickel(II) (**2**) reveal C-H···Ni anagostic interactions arising from the interaction of two non-equivalent molecules.
FTIR and NMR spectroscopy data show how electron density about the NCS_2 moiety is modified upon coordination of the ligand to the nickel metal centre. The nickel complex decomposes at ~330 °C in a single step, as shown by the TGA data. Upon heating, nickel(II) sulfide is produced, which upon examination using SEM and EDX spectroscopy revealed NiS nanowires.

Supplementary data

CCDC 1440730 contains the supplementary crystallographic data for this paper. These data can be obtained free of charge via http://www.ccdc.cam.ac.uk/conts/retrieving.html (or from the Cambridge Crystallographic Data Centre, 12, Union Road, Cambridge CB2 1EZ, UK; fax: +44 1223 336033)

Acknowledgements

We thank Dr. Ronald Shimmon for laboratory assistance, Mr Jean-Pierre Guerbois for assistance with TGA, and Dr Katie McBean for assistance with SEM.

References

[1] A.A. Aly, A.B. Brown, T.M.I. Bedair, E.A. Ishak, Journal of Sulfur Chemistry, 33 (2012) 605-617.
[2] T. Yoshimura, Y.Kotake, Antioxidants and Redox Signalling, 6 (2004) 639-647.
[3] J.J. Steggerda, J.A.Cras, J. Willemse, Recueil des Travaux Chimiques des Pays-Bas, 100 (1981) 41-48.
[4] M.N. Kouodom, G. Boscutti, M. Celegato, M. Crisma, S. Sitran, D. Aldinucci, F. Formaggio, L. Ronconi, D. Fregona, J Inorg Biochem, 117 (2012) 248-260.

[5] R.F. Borch, J.C. Katz, P.H. Lieder, M.E. Pleasants, Proc Natl Acad Sci U S A, 77 (1980) 5441-5444.
[6] K. Saito, M.Kohno, Analytical Biochemistry, 349 (2006) 16-24.
[7] G.S. Sivagurunathan, K.Ramalingam, C. Rizzoli, Polyhedron, 65 (2013) 316-321.
[8] R.S. Mane, C.D.Lockhande, Materials Chemistry and Physics, 65 (2000) 1-31.
[9] D.C. Onwudiwe, C.A. Strydom, O.S. Oluwafemi, E. Hosten, A. Jordaan, Dalton Trans, 43 (2014) 8703-8712.
[10] T. Mthethwa, V.S.R.R. Pullabhotla, P.S. Mdluli, J.W. Smith, N. Revaprasadu, Polyhedron, 28 (2009) 2977-2982.
[11] M. Lazell, S.K.Norager, P.O'Brien, N. Revaprasadu, Materials Science and Engineering: C, 16 (2001) 129-133.
[12] D.C. Onwudiwe, P.A. Ajibade, B. Omondi, Journal of Molecular Structure, 987 (2011) 58-66.
[13] P.C. Healy, J.W. Connor, B.W. Skelton, A.H. White, Aust. J. Chem, 1990 (1990) 1083-1095.
[14] M. Ito, H. Iwasaki, Acta Crystallogr B, 36 (1980) 443-444.
[15] H. Iwasaki, M. Ito, Acta Crystallogr B, 35 (1979) 2720-2721.
[16] T.A. Rodina, A.V. Ivanov, A.V. Gerasimenko, O.V. Loseva, O.N. Antzutkin, V.I. Sergienko, Polyhedron, 40 (2012) 53-64.
[17] Bruker, SADABS, in: Madison (Ed.), Bruker AXS Inc, Wisconsin, USA, 2001.
[18] Bruker, Apex2 and Saint, in: Madison (Ed.), Bruker AXS Inc, Wisonsin, USA, 2007.
[19] G.M. Sheldrick, Acta Crystallogr A, 64 (2008) 112-122.
[20] O.V. Dolomanov, L.J.Bourhis, R.J. Gildea, J.A.K. Howard, H. Puschmann, Journal of Applied Crystallography, 42 (2009) 339-341.
[21] C.F. Macrae, P.R. Edgington, P. McCabe, E. Pidcock, G.P. Shields, R. Taylor, M. Towler, J. van de Streek, Journal of Applied Crystallography, 39 (2006) 453-457.
[22] L.A. Shinobu, S.G.Jones, M.M. Jones, Acta Pharmacol Toxicol, 54 (1984) 189-194.
[23] P.W.G. Newman, .A.H. White, J.C.S Dalton, DOI (1972) 2239-2243.
[24] M. Brookheart, M.L.H. Green, G. Parkin, Proceedings of the National Academy of Sciences of the United States of America, 104 (2007) 6908-6914.
[25] J. Ruiz, J.Lorenzo, C. Vicente, G. Lopez, J.M.L de Luzuriaga, M. Monge, F.X. Aviles, D. Bautista, V. Moreno, A. Laguna, Inorganic Chemistry, 47 (2008) 6990-7001.
[26] M. Brookheart, M.L.H. Green, G. Parkin, Journal of Organometallic Chemistry, 250 (1983) 395-408.
[27] A. Husain, S.A.A. Nami, S.P. Singh, M. Oves, K.S. Siddiqi, Polyhedron, 30 (2011) 33-40.
[28] N. Ding, J.Zhang, T.S. Andy-Hor, Dalton Trans, DOI (2009) 1853-1858.
[29] B. A. Prakasam, M. Lahtinen, A. Peuronen, M. Muruganandham, E. Kolehmainen, E. Haapaniemi, M. Sillanpää, Inorganica Chimica Acta, 425 (2015) 239-246.
[30] F. Bonati, R.Ugo, Journal of Organometallic Chemistry, 10 (1967) 257-268.
[31] K. Nakamoto, J. Fujita, R.A. Condrate, Y. Morimoto, The Journal of Chemical Physics, 39 (1963) 423.
[32] A.B.P. Lever, Inorganic Electronic Spectroscopy, Elsevier 1984.
[33] R. Dingle, Inorganic Chemistry, 10 (1971) 1141-1144.
[34] S.C. Bajia, A. Mishra, Journal of Coordination Chemistry, 64 (2011) 2727-2734.
[35] W.W.H. Wong, D.E. Phipps, P.D. Beer, Polyhedron, 23 (2004) 2821-2829.
[36] V.T. Yilmaz, T.K. Yazıcılar, H. Cesur, R. Ozkanca, F.Z. Maras, Synthesis and Reactivity in Inorganic and Metal-Organic Chemistry, 33 (2003) 589-605.
[37] A.N. Bhat, R.C. Fay, D.F. Lewis, A.F. Lindmark, S.H. Strauss, Inorganic Chemistry, 13 (1974) 886-892.
[38] S. Bhattacharya, B.K. Kanungo, S. Sahoo, Journal of Coordination Chemistry, 59 (2006) 371-378.
[39] R.M. Golding, P.C. Healy, P.W.G. Newman, E. Sinn, A.H. White, Inorganic Chemistry, 11 (1972) 2435-2440.
[40] H.V. Huynh, L.R. Wong, P.S. Ng, Organometallics, 27 (2008) 2231-2237.
[41] Y. Han, H.V. Huynh, G.K. Tan, Organometallics, 26 (2007) 6447-6452.

[42] R. Taylor, O. Kennard, Journal of the American Chemical Society, 104 (1982) 5063-5070.
[43] L. Ronconi, L. Giovagnini, C. Marzano, F. Bettio, R. Graziani, G. Pilloni, D. Fregona, Inorganic Chemistry, 44 (2005) 1867-1881
[44] H.L.M. Van Gaal, J.W. Diesveld, F.W. Pijpers, J.G.M. Van Der Linden, Inorganic Chemistry, 16 (1979) 3251-3260.
[45] R. Nomura, A. Takabe, H. Matsuda, Polyhedron, 6 (1987) 411-416.
[46] I. Jen-La Plante, T.W. Zeid, P. Yang, T. Mokari, Journal of Materials Chemistry, 20 (2010) 6612.